Compartmental and noncompartmental modeling of ^{13}C-lycopene absorption, isomerization, and distribution kinetics in healthy adults[1–3]

*Nancy E Moran,[4] Morgan J Cichon,[5] Kenneth M Riedl,[4,5] Elizabeth M Grainger,[4] Steven J Schwartz,[4,5] Janet A Novotny,[8] John W Erdman Jr.,[9,10] and Steven K Clinton[4,6,7]**

[4]The Ohio State University Comprehensive Cancer Center, Departments of [5]Food Science and Technology, [6]Internal Medicine-Division of Medical Oncology, and [7]The James Cancer Hospital, The Ohio State University, Columbus, OH; [8]Human Nutrition Research Center, USDA, Beltsville, MD; and Department of [9]Food Science and Human Nutrition and [10]Division of Nutritional Sciences, The University of Illinois, Urbana, IL

ABSTRACT

Background: Lycopene, which is a red carotenoid in tomatoes, has been hypothesized to mediate disease-preventive effects associated with tomato consumption. Lycopene is consumed primarily as the all-*trans* geometric isomer in foods, whereas human plasma and tissues show greater proportions of *cis* isomers.

Objective: With the use of compartmental modeling and stable isotope technology, we determined whether endogenous all-*trans*-to-*cis*-lycopene isomerization or isomeric-bioavailability differences underlie the greater proportion of lycopene *cis* isomers in human tissues than in tomato foods.

Design: Healthy men (n = 4) and women (n = 4) consumed ^{13}C-lycopene (10.2 mg; 82% all-*trans* and 18% *cis*), and plasma was collected over 28 d. Unlabeled and ^{13}C-labeled total lycopene and lycopene-isomer plasma concentrations, which were measured with the use of high-performance liquid chromatography–mass spectrometry, were fit to a 7-compartment model.

Results: Subjects absorbed a mean ± SEM of 23% ± 6% of the lycopene. The proportion of plasma *cis*-^{13}C-lycopene isomers increased over time, and all-*trans* had a shorter half-life than that of *cis* isomers (5.3 ± 0.3 and 8.8 ± 0.6 d, respectively; $P < 0.001$) and an earlier time to reach maximal plasma concentration than that of *cis* isomers (28 ± 7 and 48 ± 9 h, respectively). A compartmental model that allowed for interindividual differences in *cis*- and all-*trans*-lycopene bioavailability and endogenous *trans*-to-*cis*-lycopene isomerization was predictive of plasma ^{13}C and unlabeled *cis*- and all-*trans*-lycopene concentrations. Although the bioavailability of *cis* (24.5% ± 6%) and all-*trans* (23.2% ± 8%) isomers did not differ, endogenous isomerization (0.97 ± 0.25 μmol/d in the fast-turnover tissue lycopene pool) drove tissue and plasma isomeric profiles.

Conclusion: ^{13}C-Lycopene combined with physiologic compartmental modeling provides a strategy for following complex in vivo metabolic processes in humans and reveals that postabsorptive *trans*-to-*cis*-lycopene isomerization, and not the differential bioavailability of isomers, drives tissue and plasma enrichment of *cis*-lycopene. This trial was registered at clinicaltrials.gov as NCT01692340. *Am J Clin Nutr* 2015;102:1436–49.

Keywords: compartmental modeling, isomers, kinetics, lycopene, tracers

INTRODUCTION

The familiar red color of tomatoes is provided by lycopene, which is a hydrocarbon carotenoid, of which American adults consume 4.5–6.5 mg/d (1). Increasingly, carefully controlled laboratory investigations have been characterizing diverse biological impacts of consumed phytochemicals such as lycopene (2–4), which have supported epidemiologic associations between estimated intakes of tomato products or blood lycopene concentrations and health outcomes (5–9). However, there remains much to be learned regarding the bioavailability, tissue distribution, and metabolism of lycopene as we attempt to elucidate the biological impacts in humans. The metabolism of lycopene is of particular interest because lycopene occurs in many geometric isomeric forms in the body (10, 11), a number of cleavage products have been identified in plasma (12, 13), and growing evidence suggests that the bioactivity of different isomers and metabolites may differ (4, 14–18).

The source, formation, and bioactivity of geometric lycopene isomers in blood and tissues are some of the critical uncertainties regarding lycopene metabolism (10, 11). Indeed, 60–96% of lycopene in raw- and processed-tomato food products is present as the all-*trans* isomer (19), whereas there is generally a lower

[1] Supported by a grant from the NIH National Center for Complementary and Alternative Medicine (5R21AT005166), The James Cancer Hospital's Bionutrition and Chemoprevention Fund (310684), The Ohio State University Center for Clinical and Translational Science (grant UL1TR001070 from the National Center for Advancing Translational Sciences), The Ohio State University Comprehensive Cancer Center and its Nutrient and Phytochemical Analytic Shared Resource (grant P30CA016058), and a Pelotonia postdoctoral fellowship (to NEM). Some carotenoid standards were donated by BASF and DSM.

[2] The content of this article is solely the responsibility of the authors and does not necessarily represent the official views of the National Center for Advancing Translational Sciences or the NIH.

[3] Supplemental Table 1 is available from the "Online Supporting Material" link in the online posting of the article and from the same link in the online table of contents at http://ajcn.nutrition.org.

*To whom correspondence should be addressed. E-mail: steven.clinton@osumc.edu.

Received November 20, 2014. Accepted for publication September 28, 2015.
First published online November 11, 2015; doi: 10.3945/ajcn.114.103143.

proportion of all-*trans*-lycopene in human blood (30–41%) (19, 20) and tissues (21–65%) (10, 11, 21). However, there has been much debate over the timing, mechanism, and location of lycopene isomerization. Kinetic differences have been observed that suggested that *cis*-lycopene isomers are more bioavailable from foods (22, 23), have a longer plasma half-life ($t_{1/2}$)[11] than all-*trans*-lycopene (24), and may be the preferred substrates for the β-carotene-9',10'-oxygenase enzyme (25). Of particular interest is the finding that, ≤24 h after the consumption of a single dose of ^{14}C-lycopene consisting of 92% all-*trans* isomer, the proportion of plasma all-*trans*-^{14}C-lycopene decreased to 50% (24), and other experiments have suggested that all-*trans*-to-*cis* isomerization may occur in the gastric milieu, enterocyte, or hepatocyte (26–29).

An investigation of the kinetics of isomerization during digestive and distributive processes in humans has proven difficult because of sparse isotope-labeled lycopene-tracer data, which are necessary to follow the metabolic fate of a single oral dose in vivo. Highly enriched ^{13}C-lycopene produced from tomato cell–suspension culturing methods (30, 31) provides a source of stable isotope–labeled lycopene for studies in humans. The application of pharmacologic principles with the use of physiologic compartmental kinetic modeling (32) can lead to estimates of lycopene bioavailability, tissue distribution, compartmental masses, and rates of clearance by integrating empirically obtained ^{13}C-lycopene plasma concentrations with a priori knowledge of the physiologic processes involved in lycopene assimilation (32–35). In this study, we tested the hypotheses that biolabeled ^{13}C-lycopene can be used to define lycopene and isomer kinetic variables in healthy adult men and women and that early lycopene isomer absorption and isomerization variables defined by compartmental modeling explain the enrichment of *cis*-lycopene in plasma and tissues. We use both noncompartmental and compartmental modeling approaches to analyze plasma ^{13}C-lycopene data to define ^{13}C-lycopene kinetic variables, thereby showing an informative application of stable isotope technology.

METHODS

Participants

Healthy adult men and women between 21 and 70 y of age, who were not currently taking carotenoid-containing dietary supplements, were recruited by word of mouth and met the following criteria that are indicative of a normal metabolic status and clotting ability during the enrollment screening visit: BMI (kg/m^2) between 18 and 27 (inclusive), Eastern Cooperative Oncology Group status of zero, and normal kidney function, liver function, lipids, blood counts, and clotting times as assessed by standard clinical laboratory procedures. On day 28, the complete blood count and liver-function assays were repeated. Subjects were excluded if they had a known allergy or intolerance to tomatoes, a history of nutrient malabsorption or metabolic disorders with special diet recommendations, uncontrolled hyperlipidemia (total cholesterol concentration >200 mg/dL, LDL concentration >160 mg/dL, and serum triglyceride concentrations >200 mg/dL), smoked tobacco products, had a history of endocrine disorders other than diabetes or osteoporosis that required hormone administration, took medications that interfered with dietary fat absorption, or took any complementary or alternative medication that may have interfered with carotenoid absorption or metabolism. The study was conducted in compliance with the ethical standards of and was approved by The Ohio State University Institutional Review Board (2009C0104), and written informed consent was obtained from all subjects. This trial was registered at clinicaltrials.gov as NCT01692340.

Study design and specimen collection

On enrollment, the first 2 subjects (one man and one woman) were instructed to follow a self-selected, controlled lycopene diet (10–20 mg/d) for 2 wk before consuming the ^{13}C-lycopene oral dose and to document compliance to this run-in diet with the use of a previously-described daily checklist (36). However, after these 2 subjects had completed the study, and plasma native lycopene and ^{13}C-lycopene were measured, the remaining subjects (3 men and 3 women) were instructed to follow a diet with ≤5 mg lycopene/d to enhance the ability to detect low-abundance ^{13}C-lycopene metabolic products by decreasing the circulating native lycopene in these 6 subjects. On the day of ^{13}C-lycopene dosing (day 0), fasted subjects reported to the Clinical Research Center and provided a baseline blood sample. Subjects consumed the test meal of 10.2 mg ^{13}C-lycopene in oil (details below) on an English muffin, which was followed by a low-carotenoid breakfast (either standard or vegetarian) (**Supplemental Table 1**) that provided 15–15.5 g fat, 20–22 g protein, and 66–68 g carbohydrate. Blood was drawn hourly (21 mL) for 10 h after dosing, and there were fasted blood draws 1, 3, and 28 d after dosing to follow the absorption, distribution, isomerization, and clearance kinetics over what a previous report indicated to be ~5 plasma lycopene-clearance half-lives (24). Blood samples were collected into evacuated tubes coated with EDTA (BD) under subdued lighting and transported on ice for centrifugation (1000 × *g*, 10 min, 4°C), plasma was collected under red light, and samples were immediately stored at −80°C. Subjects had free access to water for the rest of the day and had a low-carotenoid snack (11 g fat, 16 g protein, and 43 g carbohydrate) 3 h after dosing and a lunch (20–22 g fat, 10–24 g protein, and 48–59 g carbohydrate) 5 h after dosing. Subjects consumed a standard daily multivitamin (One Daily; CVS) for the duration of the study with the exception of the day of ^{13}C-lycopene test-meal consumption. Subjects were asked to discontinue taking any dietary nutrients or botanical supplements and were provided with a daily multivitamin to ensure an adequate nutrient status across subjects. The multivitamin provided ~100% of the US Food and Drug Administration Daily Value for most micronutrients and 2500 IU vitamin A with 80% from retinyl acetate and 20% from β-carotene, which was 50% of the Daily Value. Participants were instructed to abstain from lycopene-containing foods for the evening meal after the ^{13}C-lycopene test dose and to follow a lycopene-controlled diet (which provided 10–20 mg lycopene/d from foods) for the next

[11] Abbreviations used: C_{max}, maximal plasma ^{13}C-lycopene concentration; FSD, fractional SD; FTC, fractional transfer coefficient; MS, mass spectrometry; MtBE, methyl *tert*-butyl ether; PDA, photodiode array; T_{max}, time to reach maximal plasma concentration; $t_{1/2}$, half-life.

4 wk. Participants self-selected lycopene-containing foods to incorporate into their diets and recorded all lycopene consumption for the duration of the study with the use of a previously described lycopene-intake tracking worksheet (36). Any adverse events or unintended effects were evaluated by the study staff with the use of the National Cancer Institute's Common Terminology Criteria for Adverse Events, version 4.0, and were reported when appropriate to the Ohio State University Institutional Review Board as required.

^{13}C-Lycopene dose

Isotopically labeled lycopene was produced and isolated from tomato cell suspension cultures as previously described (30). Biolabeling yielded a distribution of mass isotopologues, and ^{13}C-lycopene was of 91% ^{13}C atomic purity and 30% uniformly labeled (**Figure 1**) as determined with the use of HPLC–mass spectrometry (MS) as previously described (30). On the morning of dosing, ~10.2 mg ^{13}C-lycopene [an amount similar to that provided by a 0.5-cup (132-g) serving of tomato-based pasta sauce or a 6-fl oz (177 mL) serving of tomato juice (~16 mg lycopene in each) (37)] was dissolved in submicron-filtered methylene chloride (7.5 mL) and mixed with 10.2 mL light (carotenoid-free) olive oil (Pompeian Extra Light Olive Oil; Pompeian Inc.) under subdued lighting. The mixture was warmed to 40°C, and methylene chloride was removed under a stream of nitrogen. A lyophilizer was used to briefly expose the sample to reduced pressure, and the removal of methylene chloride was confirmed gravimetrically as previously described (38–40). The ^{13}C-lycopene in oil and an olive-oil rinse of the dose container were transferred (final olive-oil mass: 13.65 g; 1 tablespoon) onto an English muffin (Thomas' Original; Bimbo Bakeries) and served under subdued lighting. Any residual lycopene that was not ingested was collected, quantitated, and

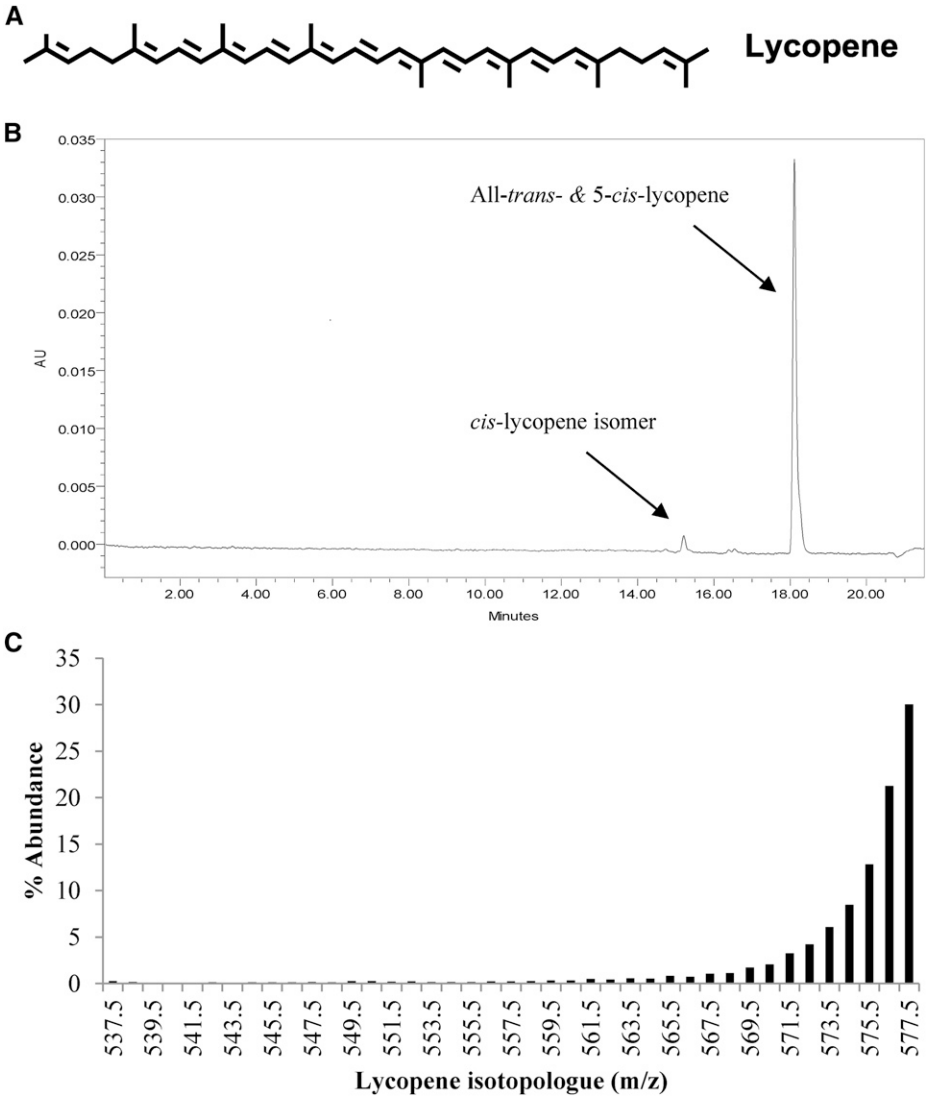

FIGURE 1 Structure of lycopene (A), representative chromatogram of ^{13}C-lycopene monitored at 470 nm (B), and the calculated ^{13}C-isotopologue distribution in ^{13}C-lycopene used for dosing (C). The percentage of isotopologue abundance was calculated from mass chromatogram peak areas of all-*E* + 5-*Z*-lycopene isotopologues masses from an $m/z = 535.5$ (the mass of unlabeled lycopene + 1 mass unit for H^+ as a result of the analysis being conducted in positive ion mode) to $m/z = 577.5$ (the mass of uniformly labeled ^{13}C-lycopene + 1 mass unit for H^+ as a result of the analysis being conducted in positive ion mode). AU, arbitrary units.

accounted for in subsequent kinetic analyses. The delivered ^{13}C-lycopene in oil masses was recorded, samples of each dose were retained for analysis, and a portion of each ^{13}C-lycopene dose was reserved before mixing with oil for use in standard calibration curves for plasma ^{13}C-lycopene analyses. Subjects consumed the dose in <10 min, and breakfast was completed <20 min after dose ingestion. The timing for blood draws began after dose ingestion.

^{13}C-Lycopene dose mass confirmation and isomeric profile analysis

The mass of ^{13}C-lycopene delivered in the dose was confirmed by a HPLC–photodiode array (PDA) analysis with the use of an authentic all-*trans*-lycopene standard (isolated in-house) for calibration. The system consisted of a Waters 2695 pump system with a Waters 996 PDA detector and a YMC C30 column (3 μm; 4.6 × 250 mm) (Waters Corp.) held at 35°C. The mobile phase consisted of A [60% methanol, 35% methyl *tert*-butyl ether (MtBE), 5% of 2% aqueous ammonium acetate, and 0.05% triethanolamine)] and B (78% MtBE, 20% methanol, 2% of 2% aqueous ammonium acetate, and 0.05% triethanolamine) applied at 1.3 mL/min beginning with 0% B and was linearly increased to 35% B over 9 min and to 100% B over 6.5 min, after which 100% B was held for 2.5 min, and conditions were returned to 0% B over 3.5 min.

Extraction and HPLC-MS analysis of plasma native and ^{13}C-lycopene

Lycopene was extracted from 1 mL plasma by mixing with 1 mL ethanol containing 0.1% (weight:volume) butylated hydroxytoluene and 5 mL hexane:ethanol:acetone:toluene solvent mixture (10:6:7:7; volume:volume:volume:volume) followed by brief probe sonication (Fisher Scientific Model 150I, immersion probe 4C15; Fisher Scientific). After centrifugation (2000 × *g* for 2 min at ambient temperature), the upper phase was reserved and the lower phase was re-extracted with 5 mL hexane:ethanol:acetone:toluene solvent mixture and centrifuged, and the upper layers were pooled and evaporated under a stream of nitrogen to dryness. Native and ^{13}C-lycopene isomers were separated and analyzed by HPLC-MS. Samples were reconstituted in 300 μL MtBE:methanol (1:1) and centrifuged (21,130 × *g* for 2 min at ambient temperature), the supernatant fluid was transferred to an autosampler vial, and 20 μL was injected. Native and ^{13}C-lycopene isomers were separated and analyzed by HPLC-MS with the use of the HPLC system previously described and interfaced with a Q-ToF Premier hybrid mass spectrometer (Micromass UK Ltd.) via an atmospheric pressure chemical ionization probe operated in negative-ion mode. Additional MS variables were as follows: corona current, 30 μA; collision energy, 8 eV; cone voltage, 40 V; source block temperature, 110°C; probe temperature, 600°C; and desolvation gas flow, 400 L/h. All MS experiments were run in Enhanced Duty Cycle mode for increased sensitivity with V-optics enabled (7500 mass resolution). The mobile phases were slightly modified to maximize the MS sensitivity (A: 60% methanol, 35% MtBE, and 5% water; B: 78% MtBE, 20% methanol, and 2% water) and were eluted as previously described. HPLC and MS data were acquired with the use of MassLynx software (v. 4.1; Waters Corp.). Plasma ^{13}C-lycopene concentrations were calculated from the peak area of ^{13}C-lycopene in plasma at the monoisotopic mass of uniformly labeled lycopene ($^{13}C_{40}H_{56}$ *m/z*: 576.57) (the ^{13}C-lycopene isotopologue distribution is shown in Figure 1) with the use of an external calibration curve of ^{13}C-lycopene. Total (native plus tracer) plasma lycopene concentrations were determined by PDA with the use of an unlabeled lycopene-calibration curve. Although native lycopene could be identified and distinguished from ^{13}C-lycopene by the accurate mass, because of the saturation of the MS response, native plasma lycopene was calculated to be the difference between total lycopene determined by PDA and ^{13}C-lycopene determined by MS. Lycopene-isomer identities were assigned on the basis if the retention time, accurate mass, and characteristic UV-visible spectra (19, 41).

Primary kinetic variable data analysis

The mean time to reach maximal plasma concentration (T_{max}) and the mean maximal plasma ^{13}C-lycopene concentration (C_{max}) were calculated from the observed values of all 8 subjects because the kinetics did not consistently differ between the first 2 subjects and the last 6 subjects. The plasma ^{13}C-lycopene AUC was calculated with the use of the log-linear trapezoidal rule (34).

Physiologic compartmental model of lycopene kinetics

The compartmental modeling approach was conducted in 2 main stages. In the first stage, the data for total lycopene were modeled on the basis of the previously published lycopene model of Diwadkar-Navsariwala et al. (32). In the second stage, a model was developed for the *cis* and all-*trans* isomers on the basis if the total lycopene model constructed in the first stage. Compartmental modeling calculations were performed with the use of WinSAAM software (v. 3.0.8; NIH, www.winsaam.com).

Compartmental modeling of total lycopene kinetics

Physiologic compartmental modeling was used to define the kinetics of ^{13}C-lycopene over 28 d. In physiologic compartmental modeling, a compartment represents a kinetically homogenous amount of material (34) and can relate to a particular body pool such as lycopene in liver, or it can represent several physiologic spaces such as lycopene in extrahepatic tissues. These compartments are connected by differential equations to represent the transfer of material between compartments, which may consist of several processes occurring in the same, kinetically distinct time frame (34). In this study, the movement of lycopene between compartments was expressed as a fraction per day, and the variables describing that movement are called fractional transfer coefficients (FTCs). FTCs are kinetic constants that describe the fraction of analyte transferred from a donor compartment (*J*) to a recipient compartment (*I*) per unit of time and are referred to as *L*(*I*,*J*) in WinSAAM modeling notation. The flow rate of analyte between compartments *J* and *I* is calculated as the product of the *L*(*I*,*J*) and the mass of analyte in the donor compartment, which results in the mass transferred per unit time (32). Initial FTCs in the total lycopene compartmental model were based on those reported previously (32) and were adjusted within physiologic constraints on the basis of the carotenoid and lipid metabolism literature until the model-predicted

data visually fit the experimentally observed data. At that point, the least-squares iterative fitting process was used to arrive at a final model for each subject, in which the model fractional SDs (FSDs) for each variable were deemed acceptable when <0.5, and the correlation between variables was generally <80%. The bioavailability of lycopene across dietary sources and from the ^{13}C-lycopene in oil was determined by the compartmental model by simultaneously analyzing labeled and unlabeled plasma lycopene data. Bioavailability was determined from the compartmental model by solving for the percentage of lycopene entering the gastrointestinal tract (through the gastrointestinal delay compartment preceding the enterocyte compartment) instead of being irreversibly lost from the gastrointestinal tract. Differences in the run-in diet protocol were not deemed to consistently affect the variables; thus, the population kinetic variables that were based on all 8 subjects were estimated with the use of a WinSAAM population analysis.

The initial model was identical to a previously published 7-compartment model describing the absorption, distribution, and clearance of lycopene (32) with exception that lycopene was modeled to be irreversibly lost from the slow-turnover tissue compartment rather than from the plasma lipoproteins (**Figure 2**). This change was made to more-accurately represent the location from which lycopene is eliminated because carotenoid cleavage enzymes are expressed in tissues (25, 42). This initial model structure fitted the empirical data well, and therefore, the structure was not changed although some variables and model constraints were modified (as later described). Subjects' average native plasma lycopene masses in the total plasma pool were calculated on the basis of HPLC-PDA analyses and plasma volumes and were included to ensure that the model predictions were conducive to maintaining the observed plasma native lycopene concentrations.

The masses of lycopene estimated to be in the fast- and slow-turnover tissue compartments at initial conditions were based on those previously published, which were calculated from human biopsy and cadaver tissue lycopene-concentration data from multiple studies and with the use of estimated tissue masses (43). The fast-turnover tissue lycopene compartment represents any extravascular lycopene that is rapidly cleared from chylomicrons and recycled to and from the plasma as lipoproteins and is generally assumed to largely reside in the liver, and thus, the initial pool-size estimate for men and women was calculated as 6.4 and 5 μmol, respectively. The slow-turnover tissue lycopene pool can be interpreted as a kinetically slower compartment that exchanges lycopene with plasma lipoproteins later than the fast turnover pool does and more slowly and is the compartment from which lycopene is irreversibly lost. The slow-turnover compartment is conceptualized to primarily represent adipose tissue but could include any other slow-turnover extravascular pool of lycopene and, thus, was initially estimated to be 21.8 μmol in men and 24.4 μmol in women (43). These compartment masses were used both as initial conditions and to evaluate the ability of the model to predict physiologically plausible tissue pool sizes. Initial estimates for the average daily intake of native lycopene included in the tracee (unlabeled lycopene from the diet) model were determined from lycopene-intake records reported from each subject.

The data used for model fitting included the ^{13}C-lycopene in plasma, the native lycopene in plasma, selected FTCs obtained from the model of Diwadkar-Navsariwala et al. (32), and kinetic data related to chylomicron clearance (44). Data related to FTCs obtained from the model of Diwadkar-Navsariwala et al. (32) were necessary because our limited plasma ^{13}C-lycopene–concentration data between days 3 and 28 could not accurately characterize tissue-to-plasma lycopene recycling when these tissue-exchange variables were loose as in the initial model. Therefore, the tissue-uptake and -clearance variables were constrained from the initial model reported to ensure physiologically relevant model predictions by incorporating the FTCs and statistical constraints calculated for the subset of men who consumed 10 mg lycopene in the Diwadkar-Navsariwala et al.

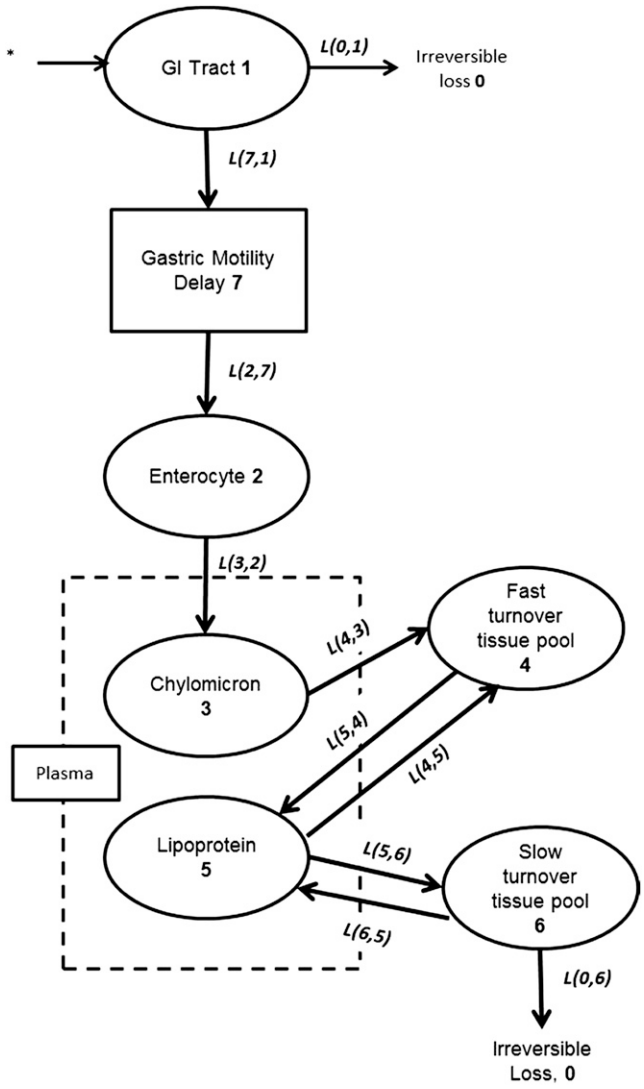

FIGURE 2 Conceptual compartmental pharmacokinetic model of total lycopene absorption, distribution, and clearance on the basis of Diwadkar-Navsariwala et al. (32). Ovals represent kinetically homogeneous, physiologic compartments. The empirically measured plasma compartment within the plasma compartment is delineated by a dashed rectangle. The rectangle enclosing "Gastric Motility Delay" represents a delay element to account for the interindividual variability in the time between ingestion and plasma appearance. ^{13}C-lycopene tracer introduction is denoted by an asterisk, bold numbers inside ovals represent compartment numbers used in the compartmental analysis, italicized lettering next to arrows represents the *L*(*I*,*J*), which is the fractional transfer coefficient, used in the model development to describe the rate of transfer between compartments for the transfer of lycopene from compartment *J* to compartment *I*. GI, gastrointestinal.

study [*L*(6,7): 0.32, FSD: 0.23; *L*(7,6): 9.24, FSD: 0.49; and *L*(7,0): 0.0167, FSD: 0.55] (32). The use of these variables from the 10-mg subset group provided narrower initial variable constraints and permitted greater certainty (FSD <0.5 and variable correlation <0.8) for the tissue related kinetic variables. Subject plasma ^{13}C-lycopene concentrations were converted to the fraction of ingested dose in the whole plasma compartment by multiplying the concentration by the total estimated plasma volume that was calculated as previously described (32), and native plasma lycopene concentrations were converted to total plasma lycopene masses by multiplying by the estimated plasma volume. Without the inclusion of the data of the average native plasma lycopene mass in the model, the estimated slow-turnover tissue lycopene pool size was unreasonably large. Exact times of blood draws were used. Some adjustments to the initial variables of the 7-compartment model published by Diwadkar-Navsariwala et al. (32) were necessary to improve the predicted fits to the observed data. Initially, the mean ± SEM chylomicron-clearance rate was estimated as $t_{1/2}$ = 16.7 ± 9.8 min because this was the variable used by Diwadkar-Navsariwala et al. (32), but the initial variable estimate was adjusted to $t_{1/2}$ = 7.1 ± 0.7 [*L*(4,3): 140.5, FSD: 0.33] on the basis of a report of chyomicron clearance in healthy adults who were fed olive oil (45), which was the oil carrier for the ^{13}C-lycopene provided to the current subjects. Other variables were adjusted to improve the physiologically plausible estimates of the absorptive and distributive kinetic variables.

Modeling of lycopene isomers

To study the absorption and interconversion kinetics of *cis*- and all-*trans*-lycopene, the model to describe total ^{13}C-lycopene kinetics was modified by constructing 2 parallel models for *cis*- and all-*trans*-lycopene (**Figure 3**), each of which were identical in structure to the final model for total lycopene. All FTCs were fixed to be equal to the final FTCs for each subject for the total lycopene compartmental model, with the exception of the bioavailability term and terms to describe all-*trans*-to-*cis* isomerization, which was tested in several pools (enterocyte, fast turnover tissue, and slow-turnover tissue lycopene compartments). Adjustments for bioavailability and isomerization (the transfer of all-*trans*-lycopene to *cis*-lycopene) were made until the tracer (labeled lycopene) and tracee (unlabeled lycopene) model predictions were in agreement with the empirical data. The percentages of labeled and unlabeled lycopene isomers absorbed were calculated with the use of WinSAAM as previously described for total lycopene.

Initially, the data used for model fitting included only plasma ^{13}C-all-*trans*-lycopene and ^{13}C-*cis*-lycopene concentrations. With

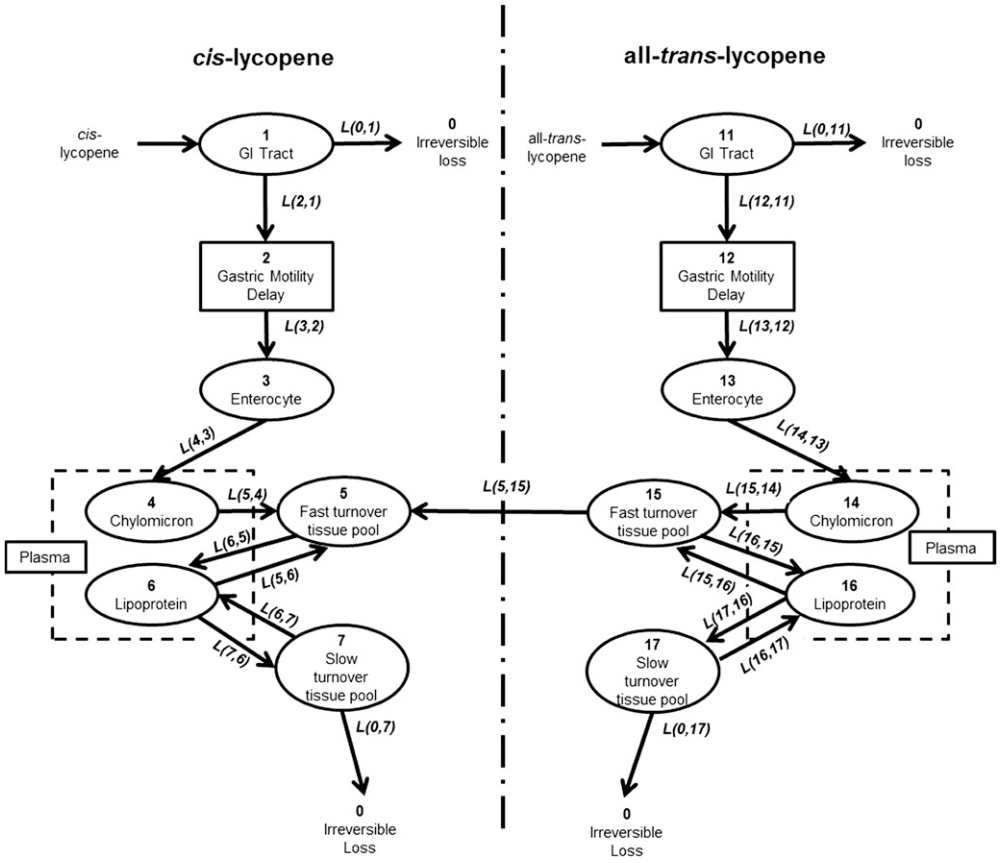

FIGURE 3 Final compartmental model describing all-*trans* and *cis-lycopene* absorption, distribution, isomerization, and clearance kinetics. Ovals represent kinetically homogeneous, physiologic compartments. The empirically measured plasma values represent the sum of 2 model compartments as delineated by the dashed rectangles. The solid rectangles enclosing "Gastric Motility Delay" represent a delay element to account for interindividual variability in the time between ingestion and plasma appearance. ^{13}C-lycopene introduction to the system is denoted by the arrows connecting "*cis*-lycopene" and "all-*trans*-lycopene" with the GI tract compartment, bold numbers inside ovals represent the compartment number used in compartmental analysis, and italicized lettering next to arrows represents the *L*(*I*,*J*), which is the fractional transfer coefficient, used in model development to describe the rate of transfer between compartments for the transfer of lycopene from compartment *J* to compartment *I*. GI, gastrointestinal.

the use of only these data, the model could provide good fits of model-predicted plasma concentrations with experimentally measured plasma data when isomerization occurred in different locations. However, this approach revealed that the location of isomerization dramatically affected predicted concentrations of all-*trans*- and *cis*-lycopene that were accumulated in body tissues, which led to predicted concentrations in body tissues that were not in agreement with previously published reports of lycopene isomer concentrations in tissues. Therefore, to define plausible kinetic variables and the lycopene isomer distribution and concentrations in the body, more-empirical information was added to the model. Specifically, parallel tracee models of unlabeled *cis*-lycopene and all-*trans*-lycopene, which included data for unlabeled *cis*- and all-*trans*-lycopene concentrations in each subject's plasma, were incorporated into the overall model for fitting.

Estimated initial condition masses of all-*trans*- and *cis*-lycopene in the fast- and slow-turnover tissue compartments were calculated with the use of the compartment masses previously described for the total lycopene model and then by multiplying by the proportion of *cis*- and all-*trans*-lycopene previously reported in the liver (~55% *cis* and ~45% all-*trans*) and adipose tissue (61% *cis* and 39% all-*trans*) (10, 21). Initial estimates for daily intakes of native all-*trans*- and *cis*-lycopene included in the tracee model were calculated to be 80% and 20% of lycopene, respectively, on the basis of previous reports of the lycopene isomer contents of foods (19).

As with the total lycopene model, parameter values were adjusted until the model prediction was in good accord with the observed data. Final variable values were determined with the use of a least-squares fitting routine. Model FTCs, flow rates, percentages of absorption, and steady state lycopene isomer masses were calculated as described for the total lycopene model. Differences in run-in diet protocols were evaluated and were not shown to consistently affect the parameters; thus, the population kinetic parameters for all 8 subjects were estimated with the use of a WinSAAM population analysis.

RESULTS

Subjects and controlled-diet compliance

Before ^{13}C-lycopene dosing, subjects (**Table 1**) consumed a controlled lycopene diet for 2 wk (run-in period). The first 2 subjects consumed an average of 12.0 mg lycopene/d, which resulted in a mean fasted native lycopene plasma concentration of 925 nmol/L (713 and 1138 nmol/L) before test-meal consumption on day 0. After preliminary analyses of the first 2 subjects' plasma samples, the remaining 6 subjects were asked to limit their intakes to 0–5 mg lycopene/d during the run-in–diet period to facilitate the detection of low amounts of lycopene cleavage products during the absorptive phase (0–10 h). These 6 subjects consumed an average of 1.3 ± 0.3 mg lycopene during the run-in period, which resulted in a fasted plasma lycopene concentration of 486 ± 78 nmol/L. However, other than baseline plasma lycopene concentrations, noncompartmental and compartmental kinetic variables for the first 2 subjects compared with the last 6 subjects did not differ, and thus, subsequent variable calculations were performed on the pooled data from all 8 subjects. From days 1–28 after ^{13}C-lycopene dosing, all subjects were asked to consume 10–20 mg lycopene/d and reported consuming an average of 11.8 ± 0.7 mg lycopene/d, which resulted in a final native plasma lycopene concentration of 868 ± 57 nmol/L, which was an 80% increase from the average plasma concentration on day 0. Only one subject consumed less than the targeted range with an average reported intake of 9.4 mg lycopene/d. The population mean fasting plasma native-lycopene concentration (n = 8) was 0.60 ± 0.10 μmol/L on day 0 and 0.86 ± 0.06 μmol/L on day 28 (**Table 2**). Subjects reported no toxicity from the ^{13}C-lycopene dose, no adverse symptoms were reported, complete blood count analyses were normal, and liver-function variables were unchanged from enrollment to day 28 of the study.

TABLE 1
Baseline subject characteristics[1]

	Subjects		
	Women (n = 4)	Men (n = 4)	Pooled (n = 8)
Age, y	26 ± 2	23 ± 2	24 ± 1
Body mass, kg	55 ± 1	79 ± 2	66 ± 5
BMI, kg/m^2	21 ± 1	24 ± 0.2	23 ± 1
Total cholesterol, mg/dL	165 ± 13	156 ± 16	160 ± 10
LDL, mg/dL	88 ± 10	92 ± 11	90 ± 7
HDL, mg/dL	64 ± 8	52 ± 7	58 ± 6
Triglycerides, mg/dL	50 ± 3	67 ± 17	58 ± 9

[1]All values are means ± SEMs measured at study enrollment.

Noncompartmental pharmacokinetics

Plasma ^{13}C-lycopene was first quantifiable 1–3 h after tracer ingestion and was quantifiable for the remainder of the study. All-*trans*-, 5-*cis*-, and other *cis*-^{13}C-lycopene isomers were detected in plasma (**Figure 4**A). The ^{13}C-lycopene test meal increased total circulating lycopene concentrations (native plus tracer) by up to 23% over the native-lycopene concentrations at 24 h (Figure 4B). Plasma ^{13}C-lycopene–concentration responses varied widely, with the C_{max} ranging from 81 to 223 nmol/L; however, when evaluated on the basis of the plasma ^{13}C-lycopene mass (i.e., when plasma concentrations were converted to plasma masses), the range of maximal masses (310–585 nmol) deviated less from the mean ± SEM amount (387 ± 53 nmol) (Figure 4C). Differences in all-*trans* and *cis*-lycopene kinetics were apparent in the concentration-time curves (Figure 4D, E) in which *cis*-^{13}C-lycopene plasma concentrations plateaued between days 1 and 3, whereas all-*trans*-^{13}C-lycopene concentrations decreased over this time period. The kinetic variables of all-*trans*- and *cis*-^{13}C-lycopene differed from those of total ^{13}C-lycopene, such that the maximal concentration and AUC for all-*trans*-^{13}C-lycopene were greater than for total *cis*-lycopene, the $t_{1/2}$ of all-*trans*-^{13}C-lycopene was shorter, and the all-*trans*-^{13}C-lycopene T_{max} occurred earlier than that of total *cis*-^{13}C-lycopene (Table 2). Although the proportion of *cis*-^{13}C-lycopene isomers in plasma increased over the 28 d, whether individual *cis*-^{13}C-lycopene isomers in the plasma differed from those in the dose could not be fully discerned from the chromatograms because some *cis* isomers co-eluted in several peaks during the gradient method used. Nevertheless, it was clear that the proportion of *cis* isomers relative to all-*trans* isomers increased over the 28-d period.

Physiologic-compartmental kinetics of total lycopene

The final model parameters, estimated compartmental lycopene masses, bioavailability, FTCs, and flow rates of total lycopene

TABLE 2
Noncompartmental, single-dose kinetics after oral ingestion of ^{13}C-lycopene in 8 healthy adults[1]

Analyte and parameter	Total	All-*trans*	Total *cis* isomers	5-*cis*
^{13}C-Lycopene				
C_{max}, μM	0.14 ± 0.02[2]	0.10 ± 0.02	0.04 ± 0.01	0.03 ± 0.004
T_{max}, h	30 ± 6	28 ± 7	48 ± 9	42 ± 9
AUC (0–672), μmol · h^{-1} · L^{-1}	31 ± 3	17 ± 3	11 ± 2	7 ± 1
Total AUC, %	–	55	35	23
$t_{1/2}$, d	6.2 ± 0.3	5.3 ± 0.3	8.8 ± 0.6	9.8 ± 0.8
Native lycopene				
Baseline (day 0) plasma concentration, μmol/L	0.60 ± 0.10	0.23 ± 0.05	0.33 ± 0.08	0.20 ± 0.04
Final (day 28) plasma concentration, μmol/L	0.86 ± 0.06	0.35 ± 0.03	0.45 ± 0.07	0.27 ± 0.04

[1] C_{max}, time to reach maximal plasma ^{13}C-lycopene concentration; T_{max}, time to reach maximal plasma concentration; $t_{1/2}$, half-life.
[2] Mean ± SEM (all such values).

between compartments are shown in **Tables 3–5**. Model-predicted fractions of tracer dose in the plasma, fast-turnover, and slow-turnover compartments for the population are shown in **Figure 5**C–E. A simultaneous evaluation of a parallel model of tracee kinetics showed that the model was predictive of both experimentally observed plasma ^{13}C-lycopene and unlabeled lycopene

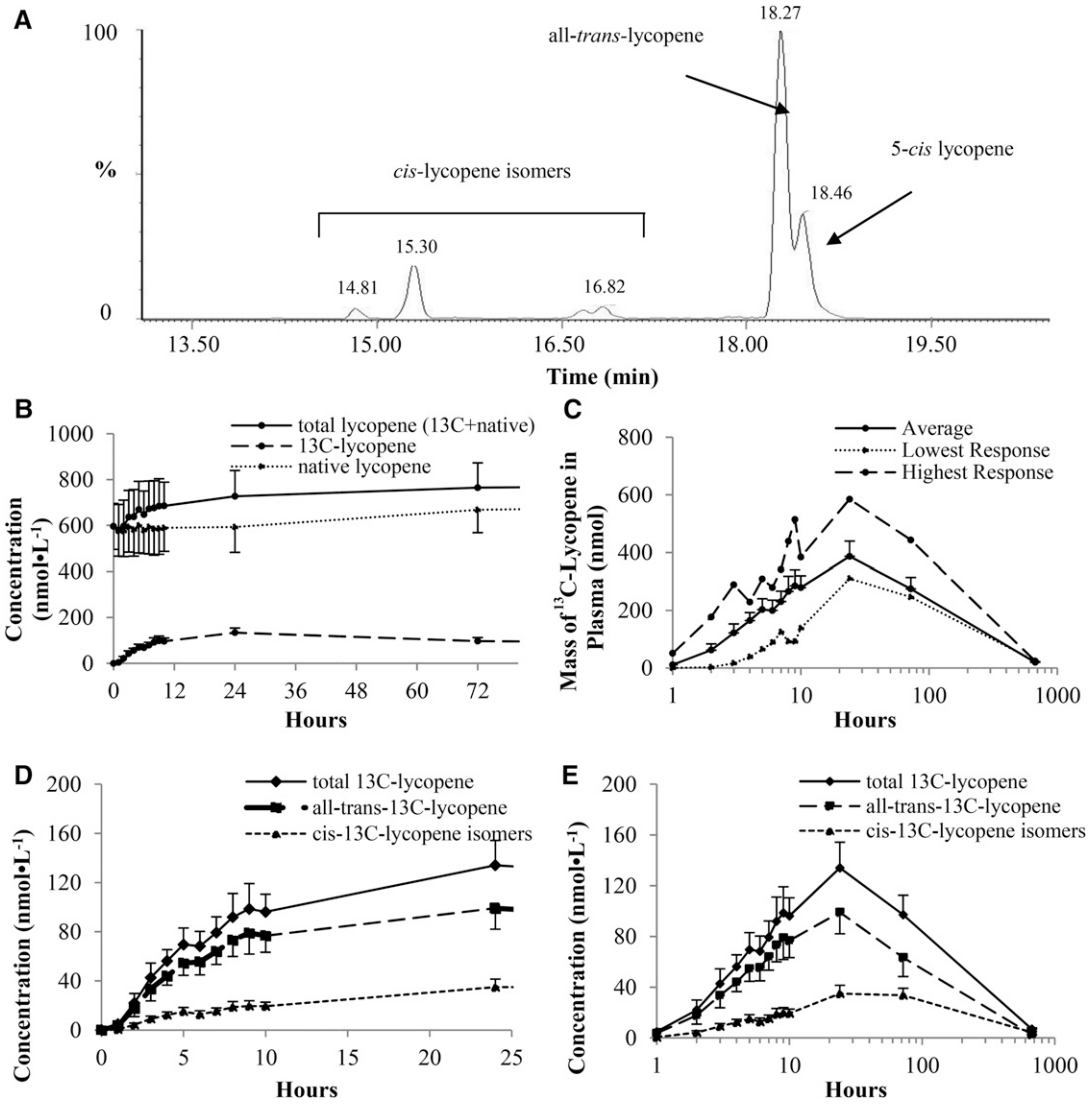

FIGURE 4 Mean ± SEM (n = 8) plasma ^{13}C-lycopene and native lycopene concentrations. (A) Extracted ion chromatogram at an m/z of 576.57 showing plasma ^{13}C-lycopene isomers. (B) Plasma native lycopene, ^{13}C-lycopene, and total (summed native and ^{13}C-lycopene) lycopene concentrations over 72 h. (C) Average, highest, and lowest plasma lycopene mass responses over 672 h. ^{13}C-lycopene isomer concentrations over 24 (D) and 672 (E) h are shown.

TABLE 3
Compartmental kinetic variables for total lycopene model[1]

From donor compartment (*n*)	To recipient compartment (*n*)	Flow rate, μmol/d	Fractional transfer coefficient, d
Gastrointestinal tract (1)	Irreversible loss (0)	11.8 ± 2.7	154.10 ± 12.92
Gastrointestinal tract (1)	Delay compartment (2)	2.46 ± 0.43	45.80 ± 12.92
Delay compartment (2)	Enterocyte (3)	2.46 ± 0.43	22.65 ± 2.78
Enterocyte (3)	Chylomicrons (4)	2.46 ± 0.43	5.51 ± 1.30
Chylomicrons (4)	Fast-turnover tissue pool (5)	2.46 ± 0.43	183.53 ± 29.48
Fast-turnover tissue pool (5)	Lipoproteins (6)	2.85 ± 0.42	1.00 ± 0.25
Lipoproteins (6)	Fast-turnover tissue pool (5)	0.40 ± 0.06	0.225 ± 0.002
Lipoproteins (6)	Slow-turnover tissue pool (7)	6.23 ± 1.12	4.05 ± 0.80
Slow-turnover tissue pool (7)	Lipoproteins (6)	3.77 ± 0.90	0.10 ± 0.04
Slow-turnover pool of tissue lycopene (7)	Irreversible loss (0)	2.46 ± 0.43	0.056 ± 0.007

[1]All values are means ± SEMs, $n = 8$.

concentrations (Figure 5A–D) along with plausible daily lycopene intakes (14.2 ± 2.6 μmol; 7.6 ± 1.4 mg).

Physiologic-compartmental kinetics of all-*trans*- and *cis*-lycopene isomers

To determine whether *cis*- and all-*trans*-lycopene have similar or dissimilar absorption, distribution, and clearance kinetic behaviors, the final model for total lycopene was applied simultaneously to all-*trans*- and to *cis*-^{13}C-lycopene with the use of 2 parallel models, one model for *cis* and one model for all-*trans*. Data inputs were adjusted to be the amount of ingested *cis*- or all-*trans*-^{13}C-lycopene and included data on plasma *cis*- or all-*trans*-^{13}C-lycopene concentrations.

For most subjects, the initial model closely predicted both *cis*- and all-*trans*-^{13}C-lycopene plasma concentrations during the first 24 h after ingestion. However the model-predicted values markedly deviated from the observed 3- and 28-d plasma *cis*- and all-*trans*-^{13}C-lycopene concentrations, which greatly overestimated plasma all-*trans* and underestimated *cis* unlabeled lycopene masses and overestimated the proportion of dietary lycopene present as *cis* relative to what was known to come from the red-tomato products that subjects reported consuming. Therefore, the inclusion of terms representing the isomerization of lycopene from the all-*trans* to *cis* forms was tested in compartments for the enterocytes, the fast-turnover pool, and the slow-turnover pool. First, to test the hypothesis that all-*trans*-to-*cis* isomerization occurs at a constant rate in all tissue compartments, isomerization rates were set as equal in the 3 tissue compartments. However, this adjustment led to a great underestimation of plasma all-*trans*-^{13}C-lycopene by day 28, an overestimation of tracer and tracee *cis*-lycopene in the plasma, an underestimation of *cis*-lycopene being consumed in the diet, and extremely low proportions of all-*trans*-lycopene in the slow-turnover lycopene tissue pool. Isomerization in the enterocyte alone led to reasonable predictions of tracee plasma *cis*-lycopene masses but greatly overestimated tracee all-*trans*-lycopene plasma masses and plasma tracer *cis*-lycopene while underestimating dietary *cis*-lycopene intake. Isomerization in the fast-turnover tissue compartment alone led to model overestimation of plasma unlabeled all-*trans*-lycopene, and isomerization in both the fast- and slow-turnover pools led to too rapid of depletion of tracer all-*trans*-lycopene with a simultaneous overestimation of plasma tracee all-*trans*-lycopene and an underestimation of slow-turnover tissue unlabeled all-*trans*-lycopene. Isomerization in the slow-turnover tissue compartment alone led to an overestimation of all-*trans*-lycopene in the fast-turnover pool, an overestimation of *cis*-lycopene from the diet, an underestimation of native *cis*-lycopene in the plasma, and an underestimation of all-*trans* lycopene in the slow turnover pool. However, of these different isomerization locations, isomerization in the fast-turnover pool provided the closest model fit to the observed data. Next, because many reports have suggested that the bioavailability of geometric isomers differs (10, 23, 46), all-*trans* bioavailability and *cis* bioavailability were allowed to freely differ, and this adjustment, along with isomerization that occurred in the fast-turnover tissue pool, resulted in reasonable model predictions of the observed tracer and unlabeled tracee data as well as plausible pool sizes and estimated intakes of *cis*- and all-*trans*-lycopene. Plots of the model-predicted concentrations of ^{13}C-lycopene isomers over 28 d show all-*trans* lycopene to be the predominant isomer at early time points in plasma and fast-turnover and slow-turnover tissue lycopene compartments, which shifted to *cis* isomers over time, whereas unlabeled plasma lycopene was predominantly present as *cis* isomers throughout (**Figure 6**).

The final model parameters, estimated compartmental lycopene isomer masses, bioavailability, FTCs, and flow rates of total lycopene between compartments are shown in **Tables 6–8**. Chylomicron lycopene was estimated to be mostly all-*trans*, lipoprotein lycopene was estimated to be more-evenly distributed between *cis* and all-*trans* forms, and both the fast- and slow- turnover extravascular tissue pools of lycopene were predicted to be composed of primarily *cis*-lycopene (Table 6).

TABLE 4
Steady state lycopene masses in physiologic compartments determined by compartmental modeling[1]

Compartment (*n*)	Steady state lycopene mass, μmol
Chylomicrons (4)	0.017 ± 0.004
Lipoproteins (6)	1.75 ± 0.27
Fast-turnover tissue lycopene pool (5)	3.67 ± 0.82
Slow-turnover tissue lycopene pool (7)	48.45 ± 11.13

[1]All values are means ± SEMs, $n = 8$.

TABLE 5
Additional variables for total lycopene kinetics determined by compartmental modeling [1]

Variable	Value
Gastrointestinal delay (compartment 2), h	1.22 ± 0.19
Bioavailability, lycopene absorbed, %	23 ± 6
Estimated intake of trace, μmol/d	14.2 ± 2.6

[1]All values are means ± SEMs. n = 8.

Furthermore, the compartmental model-calculated bioavailability of *cis*-lycopene was quite similar to that of all-*trans* (Table 7), and all-*trans*-lycopene was estimated to be the major form of lycopene consumed daily from the diet (71%). On the basis of the final model, in a lycopene intake steady state, the rate of all-*trans*-to-*cis*-lycopene isomerization was estimated to be ~58% of the fast-turnover all-*trans*-lycopene pool per day, which equated to 0.97 μmol/d (Table 8). Although differing rates of enzymatic cleavage and nonenzymatic degradation and, therefore, an irreversible loss of *cis* compared with all-*trans* isomers may exist, the current data set did not have enough data points during the terminal slope to define these processes.

DISCUSSION

With the use of stable isotope technology and plant cell culture, we produced sufficient ^{13}C-lycopene from tomato cell cultures and used a compartmental model of human lycopene kinetics in a novel way, to our knowledge, to investigate lycopene isomer kinetics with the use of simultaneous isotope-tracer and lycopene tracee data. We showed that a model incorporating lycopene isomerization in the fast-turnover compartment along with an individualizable variable for bioavailability of *cis*- and all-*trans*-lycopene isomers was predictive of the empirical plasma data and was in accord with reported lycopene isomer tissue distribution. In particular, the inclusion of an endogenous isomerization term could both account for differences in lycopene isomer plasma kinetics and for greater proportions of *cis*-lycopene in plasma and tissues relative to that in tomato foods.

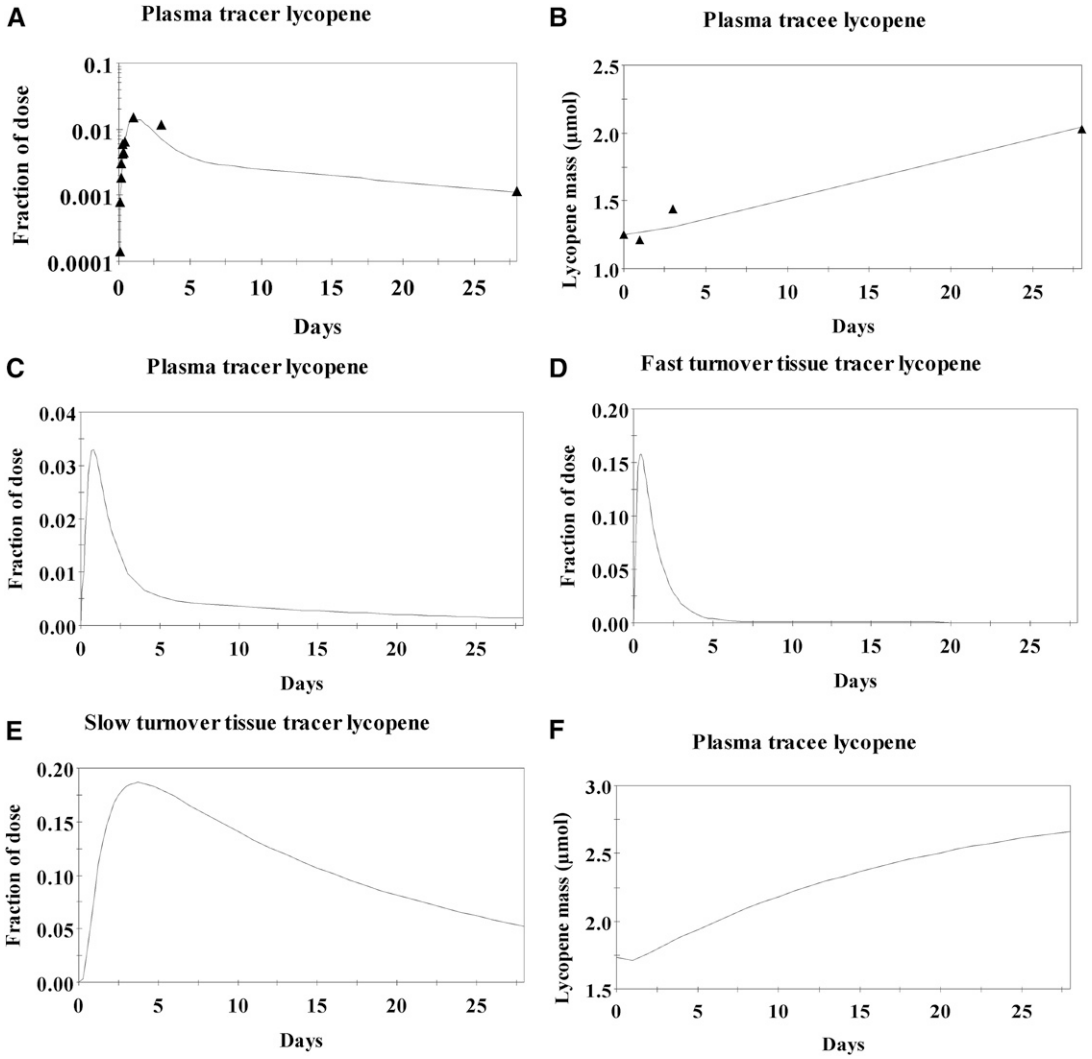

FIGURE 5 Example of total lycopene compartmental model–predicted fraction of tracer dose in plasma (A) and mass of tracee lycopene in plasma (B) in a representative subject. The solid line represents the model-predicted tracer and tracee amounts, and the solid triangles represent the empirically measured amounts. Also shown are the population averages for the fraction of the ^{13}C-lycopene dose in the total plasma compartment (C), fast-turnover (D) and slow-turnover (E) tissue lycopene pools, and the mass of tracee lycopene in the plasma (F) over 28 d after a single oral ^{13}C-lycopene dose.

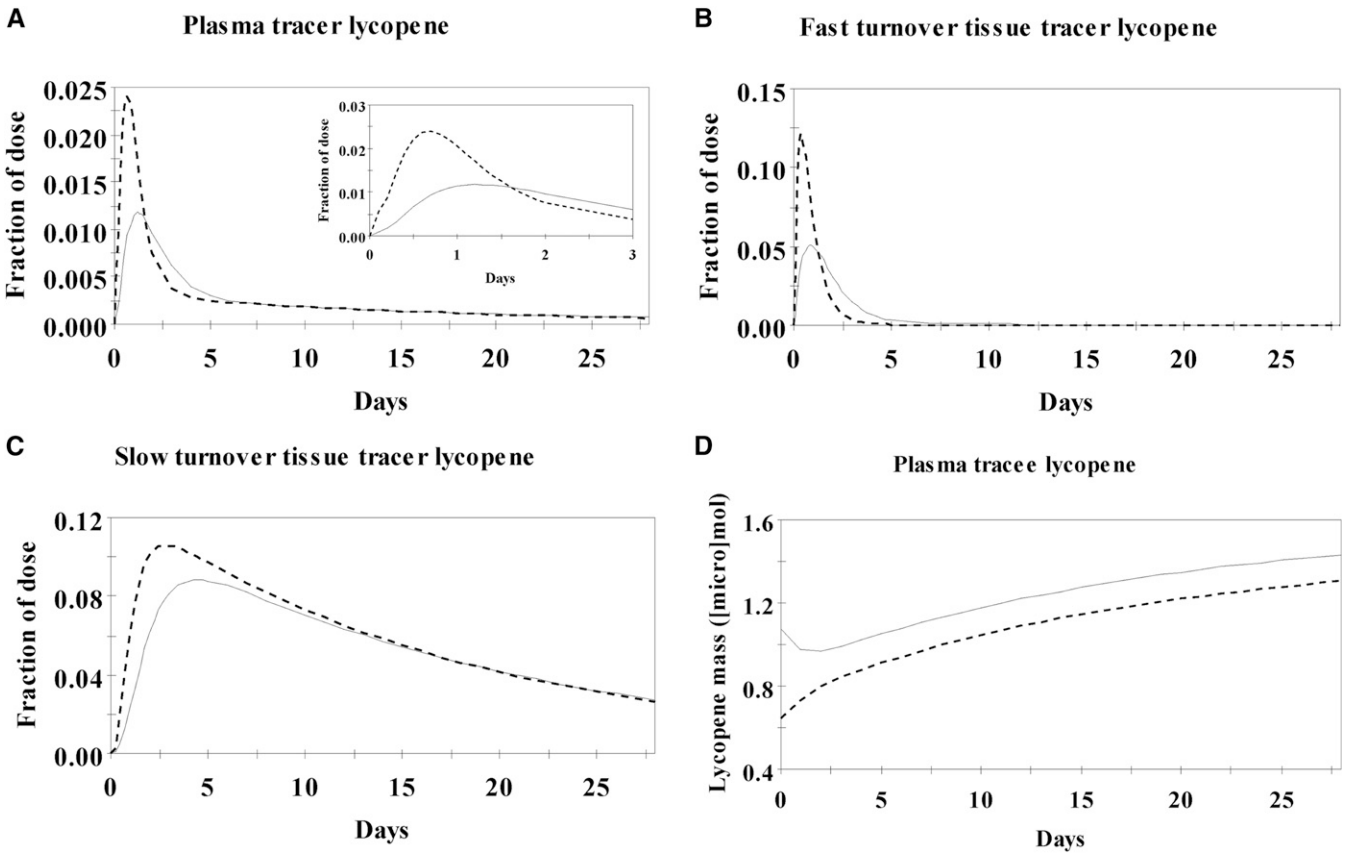

FIGURE 6 Lycopene isomer compartmental model–predicted fractions of dose in the plasma (A), fast-turnover (B) and slow-turnover (C) tissue lycopene pools, and model-predicted mass of tracee lycopene in plasma (D) over 28 d after a single oral ^{13}C-lycopene dose and during controlled dietary lycopene intakes. All-*trans* lycopene is marked with a dashed line and total *cis*-lycopene with a solid line. The inset in panel A is an enlargement of the 0–3-d fraction of dose in plasma data.

Overall, the $t_{1/2}$ and plasma responses to ^{13}C-lycopene were consistent with those previously reported for native and ^{14}C-lycopene, supporting the stable isotope strategy for detailed studies of lycopene kinetics. The total ^{13}C-lycopene $t_{1/2}$ of 6.2 ± 0.3 d was similar to the $t_{1/2}$ of 5 d previously reported for subjects who were consuming ^{14}C-lycopene (24), although it was several days longer than that in men after the consumption of lycopene from a tomato-paste beverage (47). The observed ^{13}C-lycopene T_{max} of 30 ± 6 h was more similar to the previously reported T_{max} of 17–32 h in subjects after the consumption of 10–120 mg lycopene from a tomato-paste–based beverage (47) than that reported in subjects after a ^{14}C-lycopene microdose (6 h) (24). The C_{max} of 0.14 ± 0.02 μmol/L in the current study was greater than that in subjects who consumed 5 mg ^{2}H-lycopene in corn oil (n = 2) or 10 mg ^{2}H-lycopene from intrinsically labeled tomatoes (n = 2) (0.006–0.040 μmol/L) (48), possibly because of greater label stability afforded by ^{13}C labeling compared with ^{2}H because ^{2}H may be lost from the lycopene molecule by rearrangement during metabolism or sample preparation (49). However, the C_{max} results were similar to those from individuals after the consumption of 10 and 20 mg native lycopene from a tomato-paste based beverage (0.075 and 0.16 μmol/L, respectively) (47). Differences in the C_{max} across studies that provided similar amounts of lycopene may have been due to differing amounts of oil consumed with the lycopene as suggested by previous carotenoid-absorption studies (50, 51). Four previous kinetic studies provided 9–10 mg lycopene with 0–29 g oil (24, 32, 47, 48), and the oil amount was positively correlated with the baseline-subtracted lycopene C_{max} [correlation coefficient: 0.88, P = 0.048 (Pearson correlation)].

The total ^{13}C-lycopene compartmental model kinetic parameters agreed with previous lycopene and β-carotene model

TABLE 6
Compartmental kinetic variables for all-*trans*- and *cis*-lycopene isomers[1]

Compartment	Steady state *cis*-lycopene mass, μmol (total lycopene, %)	Steady state all-*trans*-lycopene mass, μmol (total lycopene, %)
Chylomicrons	0.0035 ± 0.0008 (19)	0.015 ± 0.0045 (80)
Lipoproteins	1.12 ± 0.13 (55.5)	0.90 ± 0.17 (44.5)
Fast-turnover tissue lycopene pool	2.72 ± 0.61 (61.9)	1.68 ± 0.36 (38.1)
Slow-turnover tissue lycopene pool	30.19 ± 5.66 (59.2)	20.80 ± 4.61 (40.8)

[1]All values are means ± SEMs. n = 8.

TABLE 7
Lycopene isomer bioavailability and estimated daily intake determined by compartmental modeling [1]

	cis-Lycopene	All-*trans*-lycopene
Bioavailability, lycopene absorbed, %	24.5 ± 6.2	23.2 ± 7.6
Estimated daily intake, μmol (total lycopene, %)	3.61 ± 0.92 (28.6)	12.61 ± 2.30 (71.4)

[1]All values are means ± SEMs, n = 8.

TABLE 8
Rate of lycopene isomerization estimated by compartmental modeling[1]

	Flow rate, μmol/d	Fractional transfer coefficient, d
trans-to-*cis*-Isomerization in the fast-turnover tissue lycopene pool	0.97 ± 0.25	0.58 ± 0.10

[1]All values are means ± SEMs, n = 8.

results (32, 33), which resulted in plausible estimates of lycopene intake and tissue and plasma distributions. The absorption of lycopene in this study (23 ± 6%) was lower than that previously reported for 10 mg lycopene from a tomato-paste drink (34%) (32), which was potentially due to dose isomer-profile differences, greater accuracy resulting from the tracer distinguishability from native lycopene, dose-delivery formulation differences, or the inclusion of the unlabeled lycopene from various food sources in the model. In addition to the model's ability to predict plasma native lycopene concentrations (Figure 4), the model predictive power was shown by realistic estimates of daily lycopene intake (14.2 ± 2.6 μmol; 7.6 ± 1.4 mg), which were close to subjects' reported daily lycopene intakes (11.8 mg). Furthermore, predicted fast- and slow-turnover tissue compartment lycopene masses (3.7 and 48.5 μmol, respectively) agreed with published values (43). Thus, the ^{13}C-lycopene and native-lycopene plasma results were well characterized with the use of the previously established compartmental model.

The noncompartmental kinetic variables of all-*trans*-lycopene differed from those of *cis*-lycopene with all-*trans*-lycopene having a plasma $t_{1/2}$ of 5.5 d, whereas the combined *cis*-lycopene isomer $t_{1/2}$ was 8.8 d. These findings were very similar to the half-lives from a subject after the consumption of ^{14}C-lycopene (24) and to the half-lives of 5 and 9 d for all-*trans* and *cis*-lycopene, respectively, in subjects who consumed a tomato-containing soup or lycopene tablets (52). In addition, the later T_{max} of *cis*-lycopene than that of all-*trans*-lycopene (Table 2) was consistent with findings from men after intake of a tomato-paste–based drink (47).

Previously, several *cis*-^{14}C-lycopene isomers absent in the ^{14}C-lycopene dose given to subjects were shown in the subjects' plasma, which led the authors to propose that all-*trans*-lycopene was converted to *cis* isomers in vivo (24). Only isomerization in the fast-turnover tissue compartment was conducive to adequate predictions of plasma and tissue isomers as well as lycopene isomer intakes in the current study, which may be supported by experimental data suggesting that lycopene is isomerized in hepatic cells (27). Contrary to hypotheses suggested by previous clinical and in vitro studies (26, 47), isomerization in the enterocyte was not a major determinant of plasma isomer concentrations in this study. To reasonably predict plasma isomer concentrations, the simulations with enterocyte isomerization required very low dietary intakes of *cis*-lycopene and very low *cis*-lycopene bioavailability, both of which are in contrast to what is currently known about *cis*-lycopene intake. Isomerization in the larger, slow-turnover tissue pool was unlikely to be a major cause of isomeric profiles in the body because simulations resulted in extremely low predicted amounts of all-*trans*-lycopene in the slow-turnover pool that was interpreted to be adipose, which has nearly equal proportions of *cis*- and all-*trans*-lycopene (21). Whether endogenous all-*trans*-lycopene isomerization is primarily a thermodynamic process cannot be ascertained currently, but it is possible that the thermodynamic equilibration of all-*trans*- to *cis*-lycopene is coincident with the time frame in which lycopene passes through the fast-turnover pool before distribution to other tissues. Although carotenoid *cis* and *trans* isomerases present in plants facilitate isomerization in carotenoid biosynthesis (53), to our knowledge, there has not been a report of carotene *cis* and *trans* isomerases in animals. However, isomerization of retinal, which is a carotenoid metabolite, is a well-characterized step in the visual cycle (54). Lycopene isomerization may occur in oxidative conditions (55) that are present in the liver, which is a site of oxidative metabolism and the generation of reactive oxygen species. Whether thermodynamic equilibration, isomerases, or oxidative conditions contribute to *trans*-to-*cis* isomerization should be investigated.

In addition to isomerization, individual differences in the bioavailability of *cis*- and all-*trans*-lycopene were required in the model for good predictions of tracer and tracee *cis*- and all-*trans*-lycopene kinetics, intakes, and compartmental lycopene masses. On average the current results, in contrast with those of previous reports, did not indicate that *cis*-lycopene was more bioavailable than all-*trans* lycopene, although this finding varied between subjects. Most subjects (n = 5) absorbing a slightly greater percentage of *cis*-lycopene (16.6 ± 4.2%) than of all-*trans* lycopene (12.2 ± 2.1%), and fewer subjects (n = 3) absorbed both greater total amounts of lycopene and a somewhat greater percentage of all-*trans*-lycopene (43.7 ± 13.9%) than of *cis*-lycopene (36.6 ± 13.7%). Thus, consistent isomer-bioavailability differences did not clearly drive the greater proportion of tissue and plasma *cis*-lycopene shown in vivo. Whether interindividual lycopene-bioavailability differences result from genetic variation in transport and metabolic genes deserves additional investigation (43).

In conclusion, to our knowledge, this is the largest tracer study in men and women of lycopene kinetics to date, providing superior confidence in the observations and modeling results. Larger studies of variables believed to affect individuals' kinetic responses to lycopene may improve the specificity of the model. The FTCs, flow rates, and bioavailability in this study apply not only to the ^{13}C-lycopene but also to the unlabeled lycopene kinetic data. Therefore, the compartmental model findings may be generalizable across lycopene-containing foods. The lack of samples collected between days 3 and 28 reduced the ability to characterize differences in *cis*- and all-*trans*-lycopene tissue plasma recycling and irreversible loss. This study shows that ^{13}C-lycopene from plant cell cultures is useful for defining lycopene kinetic variables, and endogenous all-*trans*-to-*cis* isomerization is a major source of greater proportions of tissue and plasma *cis*-lycopene than that in foods.

We thank Mary Ann Lila for providing laboratory space and equipment for ^{13}C-lycopene production from tomato cell cultures, Randy B Rogers for assisting in the production and isolation of ^{13}C-lycopene from tomato cell cultures, and Lauren E Conlon for assisting in the isolation of ^{13}C-lycopene from tomato cell cultures. We also thank Michael Green for helpful discussions on the model development and evaluation.

The authors' responsibilities were as follows—NEM, MJC, KMR, EMG, and JAN conducted research; NEM, MJC, JAN, JWE, and SKC wrote the manuscript; NEM and JAN: analyzed the noncompartmental and compartmental model kinetic data; MJC and KMR: analyzed the mass spectrometric data; SKC: had primary responsibility for the final content of the manuscript; and all authors: designed the research, contributed to the interpretation of the data, and read and approved the final manuscript. Neither Pelotonia nor The James Cancer Hospital's Bionutrition and Chemoprevention Fund was involved in the design, implementation, analysis, or interpretation of the data for this publication. None of the authors reported a conflict of interest related to the study.

REFERENCES

1. US Department of Agriculture, Agricultural Research Service. Total nutrient intakes: percent reporting and mean amounts of selected vtamins and minerals from food and dietary supplements, by family inome (as % of federal poverty threshold) and age. What we eat in America, NHANES 2009-2010. c2012. Available from: www.ars.usda.gov/ba/bhnrc/fsrg.
2. Qiu X, Yuan Y, Vaishnav A, Tessel MA, Nonn L, van Breemen RB. Effects of lycopene on protein expression in human primary prostatic epithelial cells. Cancer Prev Res (Phila) 2013;6:419–27.
3. Wan L, Tan HL, Thomas-Ahner J, Pearl DK, Erdman JW Jr., Moran NE, Clinton SK. Dietary tomato and lycopene impact androgen signaling- and carcinogenesis-related gene expression during early TRAMP prostate carcinogenesis. Cancer Prev Res (Phila) 2014;7:1228–39.
4. Ford NA, Erdman JW, Jr. Are lycopene metabolites metabolically active? Acta Biochim Pol 2012;59:1–4.
5. Zu K, Mucci L, Rosner BA, Clinton SK, Loda M, Stampfer MJ, Giovannucci E. Dietary lycopene, angiogenesis, and prostate cancer: a prospective study in the prostate-specific antigen era. J Natl Cancer Inst 2014;106:djt430.
6. Giovannucci E, Ascherio A, Rimm EB, Stampfer MJ, Colditz GA, Willett WC. Intake of carotenoids and retinol in relation to risk of prostate cancer. J Natl Cancer Inst 1995;87:1767–76.
7. Giovannucci E, Rimm EB, Liu Y, Stampfer MJ, Willett WC. A prospective study of tomato products, lycopene, and prostate cancer risk. J Natl Cancer Inst 2002;94:391–8.
8. Eliassen AH, Hendrickson SJ, Brinton LA, Buring JE, Campos H, Dai Q, Dorgan JF, Franke AA, Gao YT, Goodman MT, et al. Circulating carotenoids and risk of breast cancer: pooled analysis of eight prospective studies. J Natl Cancer Inst 2012;104:1905–16.
9. Karppi J, Laukkanen JA, Makikallio TH, Kurl S. Low serum lycopene and beta-carotene increase risk of acute myocardial infarction in men. Eur J Public Health 2012;22:835–40.
10. Stahl W, Schwarz W, Sundquist AR, Sies H. cis-trans isomers of lycopene and beta-carotene in human serum and tissues. Arch Biochem Biophys 1992;294:173–7.
11. Clinton SK, Emenhiser C, Schwartz SJ, Bostwick DG, Williams AW, Moore BJ, Erdman JW Jr. cis-trans lycopene isomers, carotenoids, and retinol in the human prostate. Cancer Epidemiol Biomarkers Prev 1996;5:823–33.
12. Kopec RE, Riedl KM, Harrison EH, Curley RW Jr., Hruszkewycz DP, Clinton SK, Schwartz SJ. Identification and quantification of apolycopenals in fruits, vegetables, and human plasma. J Agric Food Chem 2010;58:3290–6.
13. Khachik F, Carvalho L, Bernstein PS, Muir GJ, Zhao DY, Katz NB. Chemistry, distribution, and metabolism of tomato carotenoids and their impact on human health. Exp Biol Med (Maywood) 2002;227:845–51.
14. Müller L, Goupy P, Frohlich K, Dangles O, Caris-Veyrat C, Bohm V. Comparative study on antioxidant activity of lycopene (Z)-isomers in different assays. J Agric Food Chem 2011;59:4504–11.
15. Chung J, Koo K, Lian F, Hu KQ, Ernst H, Wang XD. Apo-10'-lycopenoic acid, a lycopene metabolite, increases sirtuin 1 mRNA and protein levels and decreases hepatic fat accumulation in ob/ob mice. J Nutr 2012;142:405–10.
16. Mein JR, Lian F, Wang XD. Biological activity of lycopene metabolites: implications for cancer prevention. Nutr Rev 2008;66:667–83.
17. Yang CM, Hu TY, Hu ML. Antimetastatic effects and mechanisms of apo-8′-lycopenal, an enzymatic metabolite of lycopene, against human hepatocarcinoma SK-Hep-1 cells. Nutr Cancer 2012;64:274–85.
18. Yang CM, Huang SM, Liu CL, Hu ML. Apo-8′-lycopenal induces expression of HO-1 and NQO-1 via the ERK/p38-Nrf2-ARE pathway in human HepG2 cells. J Agric Food Chem 2012;60:1576–85.
19. Schierle J, Bretzel W, Buhler I, Faccin N, Hess D, Steiner K, Schuep W. Content and isomeric ratio of lycopene in food and human blood plasma. Food Chem 1997;59:459–65.
20. Allen CM, Schwartz SJ, Craft NE, Giovannucci EL, De Groff VL, Clinton SK. Changes in plasma and oral mucosal lycopene isomer concentrations in healthy adults consuming standard servings of processed tomato products. Nutr Cancer 2003;47:48–56.
21. Walfisch Y, Walfisch S, Agbaria R, Levy J, Sharoni Y. Lycopene in serum, skin and adipose tissues after tomato-oleoresin supplementation in patients undergoing haemorrhoidectomy or peri-anal fistulotomy. Br J Nutr 2003;90:759–66.
22. Stahl W, Sies H. Uptake of lycopene and its geometrical isomers is greater from heat-processed than from unprocessed tomato juice in humans. J Nutr 1992;122:2161–6.
23. Unlu NZ, Bohn T, Francis DM, Nagaraja HN, Clinton SK, Schwartz SJ. Lycopene from heat-induced cis-isomer-rich tomato sauce is more bioavailable than from all-trans-rich tomato sauce in human subjects. Br J Nutr 2007;98:140–6.
24. Ross AB, Vuong le T, Ruckle J, Synal HA, Schulze-König T, Wertz K, Rümbeli R, Liberman RG, Skipper PL, Tannenbaum SR, et al. Lycopene bioavailability and metabolism in humans: an accelerator mass spectrometry study. Am J Clin Nutr 2011;93:1263–73.
25. Hu KQ, Liu C, Ernst H, Krinsky NI, Russell RM, Wang XD. The biochemical characterization of ferret carotene-9',10'-monooxygenase catalyzing cleavage of carotenoids in vitro and in vivo. J Biol Chem 2006;281:19327–38.
26. Richelle M, Sanchez B, Tavazzi I, Lambelet P, Bortlik K, Williamson G. Lycopene isomerisation takes place within enterocytes during absorption in human subjects. Br J Nutr 2010;103:1800–7.
27. Teodoro AJ, Perrone D, Martucci RB, Borojevic R. Lycopene isomerisation and storage in an in vitro model of murine hepatic stellate cells. Eur J Nutr 2009;48:261–8.
28. Re R, Fraser PD, Long M, Bramley PM, Rice-Evans C. Isomerization of lycopene in the gastric milieu. Biochem Biophys Res Commun 2001;281:576–81.
29. Moraru C, Lee TC. Kinetic studies of lycopene isomerization in a tributyrin model system at gastric pH. J Agric Food Chem 2005;53:8997–9004.
30. Moran NE, Rogers RB, Lu CH, Conlon LE, Lila MA, Clinton SK, Erdman JW, Jr. Biosynthesis of highly enriched 13C-lycopene for human metabolic studies using repeated batch tomato cell culturing with 13C-glucose. Food Chem 2013;139:631–9.
31. Engelmann NJ, Campbell JK, Rogers RB, Rupassara SI, Garlick PJ, Lila MA, Erdman JW Jr. Screening and selection of high carotenoid producing in vitro tomato cell culture lines for [13C]-carotenoid production. J Agric Food Chem 2010;58:9979–87.
32. Diwadkar-Navsariwala V, Novotny JA, Gustin DM, Sosman JA, Rodvold KA, Crowell JA, Stacewicz-Sapuntzakis M, Bowen PE. A physiological pharmacokinetic model describing the disposition of lycopene in healthy men. J Lipid Res 2003;44:1927–39.
33. Novotny JA, Dueker SR, Zech LA, Clifford AJ. Compartmental analysis of the dynamics of beta-carotene metabolism in an adult volunteer. J Lipid Res 1995;36:1825–38.
34. Atkinson AJ Jr., Huang S-H, Lertora JJL, Markey SP. Principles of clinical pharmacology. 3rd ed. San Diego (CA): Elsevier; 2012.
35. Novotny JA. What can pharmacokinetic models tell us about the disposition of lycopene and the potential role of lycopene in cancer prevention? J Nutr 2005;135:2048S–9S.
36. Grainger EM, Schwartz SJ, Wang S, Unlu NZ, Boileau TW, Ferketich AK, Monk JP, Gong MC, Bahnson RR, DeGroff VL, et al. A combination of tomato and soy products for men with recurring prostate cancer and rising prostate specific antigen. Nutr Cancer 2008;60:145–54.
37. U.S. Department of Agriculture Agricultural Research Service. National nutrient database for standard reference release 26. Beltsville (MD): National Agricultural Library; 2013.

38. Zaripheh S, Erdman JW Jr. The biodistribution of a single oral dose of [14C]-lycopene in rats prefed either a control or lycopene-enriched diet. J Nutr 2005;135:2212–8.
39. Campbell JK, Engelmann NJ, Lila MA, Erdman JW Jr. Phytoene, phytofluene, and lycopene from tomato powder differentially accumulate in tissues of male Fisher 344 rats. Nutr Res 2007;27: 794–801.
40. Zaripheh S, Boileau TW, Lila MA, Erdman JW Jr. [14C]-lycopene and [14C]-labeled polar products are differentially distributed in tissues of F344 rats prefed lycopene. J Nutr 2003;133:4189–95.
41. Fröhlich K, Conrad J, Schmid A, Breithaupt DE, Bohm V. Isolation and structural elucidation of different geometrical isomers of lycopene. Int J Vitam Nutr Res 2007;77:369–75.
42. Redmond TM, Gentleman S, Duncan T, Yu S, Wiggert B, Gantt E, Cunningham FX Jr. Identification, expression, and substrate specificity of a mammalian beta-carotene 15,15′-dioxygenase. J Biol Chem 2001; 276:6560–5.
43. Moran NE, Erdman JW, Jr., Clinton SK. Complex interactions between dietary and genetic factors impact lycopene metabolism and distribution. Arch Biochem Biophys 2013;539:171–80.
44. Cortner JA, Coates PM, Le NA, Cryer DR, Ragni MC, Faulkner A, Langer T. Kinetics of chylomicron remnant clearance in normal and in hyperlipoproteinemic subjects. J Lipid Res 1987;28:195–206.
45. Park Y, Harris WS. Omega-3 fatty acid supplementation accelerates chylomicron triglyceride clearance. J Lipid Res 2003;44:455–63.
46. Failla ML, Chitchumroonchokchai C, Ishida BK. In vitro micellarization and intestinal cell uptake of cis isomers of lycopene exceed those of all-trans lycopene. J Nutr 2008;138:482–6.
47. Gustin DM, Rodvold KA, Sosman JA, Diwadkar-Navsariwala V, Stacewicz-Sapuntzakis M, Viana M, Crowell JA, Murray J, Tiller P, Bowen PE. Single-dose pharmacokinetic study of lycopene delivered in a well-defined food-based lycopene delivery system (tomato paste-oil mixture) in healthy adult male subjects. Cancer Epidemiol Biomarkers Prev 2004;13:850–60.
48. Tang G, Ferreira AL, Grusak MA, Qin J, Dolnikowski GG, Russell RM, Krinsky NI. Bioavailability of synthetic and biosynthetic deuterated lycopene in humans. J Nutr Biochem 2005;16:229–35.
49. van Lieshout M, West CE, van Breemen RB. Isotopic tracer techniques for studying the bioavailability and bioefficacy of dietary carotenoids, particularly beta-carotene, in humans: a review. Am J Clin Nutr 2003;77:12–28.
50. Unlu NZ, Bohn T, Clinton SK, Schwartz SJ. Carotenoid absorption from salad and salsa by humans is enhanced by the addition of avocado or avocado oil. J Nutr 2005;135:431–6.
51. Brown MJ, Ferruzzi MG, Nguyen ML, Cooper DA, Eldridge AL, Schwartz SJ, White WS. Carotenoid bioavailability is higher from salads ingested with full-fat than with fat-reduced salad dressings as measured with electrochemical detection. Am J Clin Nutr 2004;80:396–403.
52. Cohn W, Thurmann P, Tenter U, Aebischer C, Schierle J, Schalch W. Comparative multiple dose plasma kinetics of lycopene administered in tomato juice, tomato soup or lycopene tablets. Eur J Nutr 2004;43:304–12.
53. Isaacson T, Ohad I, Beyer P, Hirschberg J. Analysis in vitro of the enzyme CRTISO establishes a poly-cis-carotenoid biosynthesis pathway in plants. Plant Physiol 2004;136:4246–55.
54. Cascella M, Barfuss S, Stocker A. Cis-retinoids and the chemistry of vision. Arch Biochem Biophys 2013;539:187–95.
55. Graham DL, Carail M, Caris-Veyrat C, Lowe GM. (13Z)- and (9Z)-lycopene isomers are major intermediates in the oxidative degradation of lycopene by cigarette smoke and Sin-1. Free Radic Res 2012;46:891–902.